

Kais Brik¹

Research Laboratory Materials,
Measurements and Applications,
University of Carthage,
Centre Urbain Nord,
BP No. 676,
Tunis 1080, Tunisia
e-mail: Kais.brik@yahoo.fr

Faouzi Ben Ammar

Research Laboratory Materials,
Measurements and Applications,
University of Carthage,
Centre Urbain Nord,
BP No. 676,
Tunis 1080, Tunisia
e-mail: Faouzi.benamar@yahoo.fr

Abdesslam Djerdir

FClab,
University of Technology of Belfort-Montbéliard,
Belfort 90000, France
e-mail: abdesslem.djerdir@utbm.fr

Abdellatif Miraoui

FClab,
University of Technology of Belfort-Montbéliard,
Belfort 90000, France
e-mail: abdellatif.miraoui@utbm.fr

Causal and Fault Trees Analysis of Proton Exchange Membrane Fuel Cell Degradation

This paper presents a reliability approach to analyze the degradation of proton exchange membrane fuel cell. This approach is based on the dependability analysis tools such as the causal and fault trees to establish an analysis of the internal state of the fuel cell energy conversion performance and evaluate its lifetime. The elaboration of causal tree offers powerful tools to a deductive analysis, which consists on seeking the various combinations of events leading to the fuel cell degradation. The parameters of fuel cell model are identified in order to found the degree of degradation. The experimental determination of the variation interval of the parameters is done according to each of degradation modes. A diagnostic method is proposed in order to identify the depth of each aging process of the fuel cell. The diagnosis is done by comparing the experimental output characteristic at beginning of life of the fuel cell with the used fuel cell to qualify and quantify the depth of degradation. [DOI: 10.1115/1.4031584]

1 Introduction

Nowadays, the improvement in fuel cell systems for industrial applications has rapidly accelerated; indeed, they deliver electrical power with low operation noise and no gas emissions [1,2]. The fuel cells initiate a large domain of applications: transport, power systems, stationary fuel cell applications, and portable fuel cell applications [3]. The integration of fuel cells in industrial applications is limited by the degradation phenomena, which reduce the energy production. In fact, the fuel cell loses its performances during the cycling by the deficiency of the membrane and the electrodes. Recently, the research community of fuel cell has shown a considerable interest for diagnosis in view to ensure reliability. In the literature, several papers published different approaches of the fuel cell systems diagnosis such as the electrochemical impedance spectroscopy, the electrochemical noise, and the magnetic field [4–6]. In this paper, the authors propose to analyze the degradation depth of the fuel cell during the operation process by adopting an approach based on the dependability analysis tools.

The causal tree is a powerful deductive procedure to backwardly deduce the causes of undesirable events in proton exchange membrane fuel cell (PEMFC) failure, and it presents all possible combinations of causes and faults leading to the loss of PEMFC. The causal tree analysis (CTA) [7–9] is known as taking a top-down approach using a tree structure which is made of successive levels of events, e.g., each event is generated from the events of the lower level via various logical operators (AND, OR, XOR, etc.). The fault tree explicitly shows all the different relationships that are necessary to result in the top event (loss of PEMFC). In constructing the fault tree, a thorough understanding is obtained of the logic and basic causes (lowest level event) leading to the top event. The CTA

methodology is recognized by international standard object (UTE C 20-318. ECSS-Q-4012 CEI 1025). The main purpose of the CTA is to help identify potential causes of system failures before the failures actually occur by using technical information and professional judgments, and it can also be used to evaluate the probability of occurrence for each cause in the lowest level and calculate the probability of the top event using analytical or statistical methods. The analysis of the reliability of proton exchange membrane fuel cell consists of two parts.

In the first part, the authors develop a CTA to help and identify potential causes of fuel cell system failures. The causal tree shows all different relationships that are necessary to result in the top event described by the fuel cell system degradation. This degradation is generated by one or more auxiliary elements in the system, membrane degradation and electrode degradation.

In the second part, the authors develop a diagnostic approach using the experimental measurements of the output characteristic at the beginning of the fuel cell life. In this approach, a fault tree is developed and presents the parameters variations of the fuel cell model and their effects on degradation. Finally, the authors develop a diagnostic system to identify the degradation modes and the degradation degree of the proton exchange membrane fuel cell.

2 Degradation Analysis of Fuel Cell System

A fuel cell system requires for its operation the addition of several auxiliary elements, which ensure the provisioning of the reaction (hydrogen and air), their conditioning (pressure and flows), and the management of the products of the reaction (water, heat, and electricity). The reformer, the compressor, and the humidifiers are thus the key elements in the development of the system fuel cell [10–12]. The cycles of use decrease the fuel cell performances and create a reduction in energy production. This aging is generated by the malfunction of one or more elements in the system.

2.1 Causal Tree of Fuel Cell System. In order to be capable to produce energy, it is necessary to integrate the fuel cell stack

¹Corresponding author.

Contributed by the Advanced Energy Systems Division of ASME for publication in the JOURNAL OF FUEL CELL SCIENCE AND TECHNOLOGY. Manuscript received October 2, 2014; final manuscript received August 30, 2015; published online October 6, 2015. Assoc. Editor: Rak-Hyun Song.

with other auxiliary components to form a fuel cell-based power generation system.

These auxiliary elements of PEMFC are divided into the following subsystems:

- a compressor which feeds the cathode circuit in air.
- a feeding system in hydrogen: if hydrogen is manufactured in a place, it contains a reformer system. If not, it contains a pressure tank and a pressure reducer ensuring the adjustment of the hydrogen pressure.
- two humidifiers to humidify gases, in order to allow a correct operation of the membranes.
- various accessories intended for the distribution of gases.
- a cooling circuit that regulates the operating temperature of fuel cell system.
- a power converter that allows management of energy delivered by the fuel cell.
- a system of control ensures the management of gas flows according to the current requested and the safety of the system.

Figure 1 shows an example of fuel cell system with the different auxiliaries and presents the interrelation between the main components. The combinations of events, which lead to fuel cell system degradation, are presents in Fig. 2. In fact, the stop of operation of the fuel cell system is generally generated by the failure of the auxiliary elements, membrane degradation and electrode degradation.

2.1.1 Causal Tree of Auxiliary Elements. The operation of a fuel cell stack requires the exploitation of several auxiliary subsystems, whose function is to organize reactant feeding, heat, and water and to allow an efficient and reliable electric power production. In this context, a malfunction of one or more subsystems can stop the production of energy. The failure of the auxiliary elements shown in Fig. 3 is provided by the degradation of the compressor, the feeding system in hydrogen, the humidifier, the cooling circuit, the power converter, and the erroneous information given by the control system.

2.1.2 Causal Tree of Fuel Cell. The causal tree construction of the fuel cell is based on the study of the involving events that cause the loss of energy production. This causal tree consists of five levels of causality, which describe the various phenomena causing the reduction in the performances of the fuel cell. These losses of performances are generated by the degradation of the various parts of the fuel cell: the electrodes, the membrane, and the catalyst [13–16].

2.1.2.1 Membrane degradation. The efficiency of a fuel cell is dependent on the amount of power drawn from it. During fuel cell operation, the membrane undergoes mechanical and chemical aggressions. Indeed, it is subjected to mechanical constraints of significant compression and shearing. These constraints generate

the penetration of carbon fibers in the membrane and start short circuit. When the gases are humidified, the conductivity of the membrane is higher and the fuel cell provides a more significant voltage. When the temperature is higher than 80 °C, the operation of the fuel cell becomes delicate because of the draining membrane, and thus of the reduction in its conductivity. This draining accelerates the degradation of the membrane by the creation of porosities, which lead the passing of gases from one compartment to another. The cycling mode accelerates the degradation of the membrane by the variations in temperature, the variations of potential of the electrodes, and the successive periods of swelling.

The reduction of deoxygenize to cathode during the operation of the fuel cell involves the formation of some hydrogen peroxide molecules (H_2O_2). These molecules react with traces of metal ions present in the membrane to form radicals which are strongly oxidizing species. These radicals attack the chemical liaisons and produce a thinning of the membrane. The presence of the metal cations in the fuel cell system, in particular, in the tanks, the piping line, and the bipolar plates contaminates the membrane and generates a reduction in conductivity with an increase in its resistance. The metals employed in the bipolar plates are in contact with water, and they generate a stagnation of corrosive substances in the channels. These products cause pollution of the membrane, and the performances of the fuel cell are thus considerably affected. The causal tree of membrane degradation is illustrated in Fig. 4.

2.1.2.2 Electrodes degradation. The electrodes used in the fuel cells are impregnate of a fine layer, which ensures cohesion between the catalyst particles and the electrode. One of the present problems of the energy production by a fuel cell is the progressive poisoning of catalysts. This contamination is created by carbon monoxide present in the vapor form of hydrogen. The carbon monoxide reactant generally poisons the anode of the fuel cell and decreases the ionization speed of hydrogen. Indeed, a carbon monoxide rate higher than 10 ppm is enough to poison the anode and causes a fall of voltage. The size of platinum particles increases by both the raise of cycle's number and temperature, and generates the agglomeration. This agglomeration involves the reduction in active surface and the increase in the losses of activation. The binder is likely to be attack by the radicals and involves the detachment of the catalyst particles. Certainly, the rate of decomposition of the binder is more significant when the pressure of gases increases. The causal tree of electrode degradation is illustrated in Fig. 5.

2.2 Reliability Estimation. After the graphically creation of the causal tree of the fuel cell system, it is important to estimate its reliability.

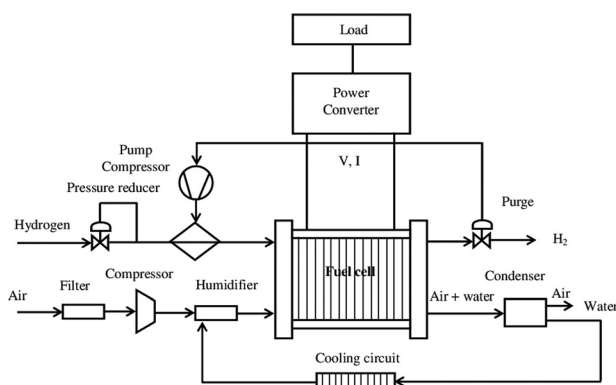


Fig. 1 Fuel cell system

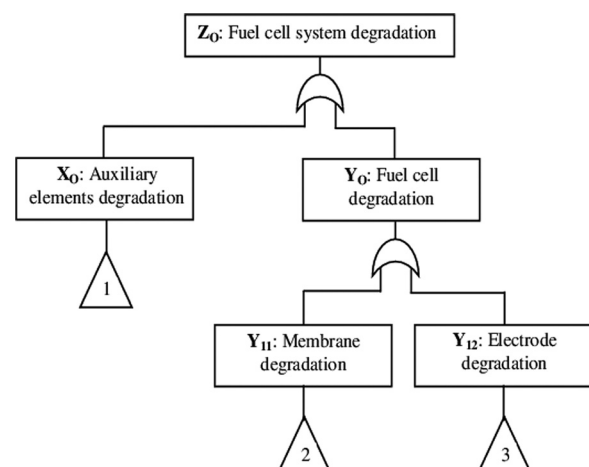


Fig. 2 Causal tree of fuel cell system

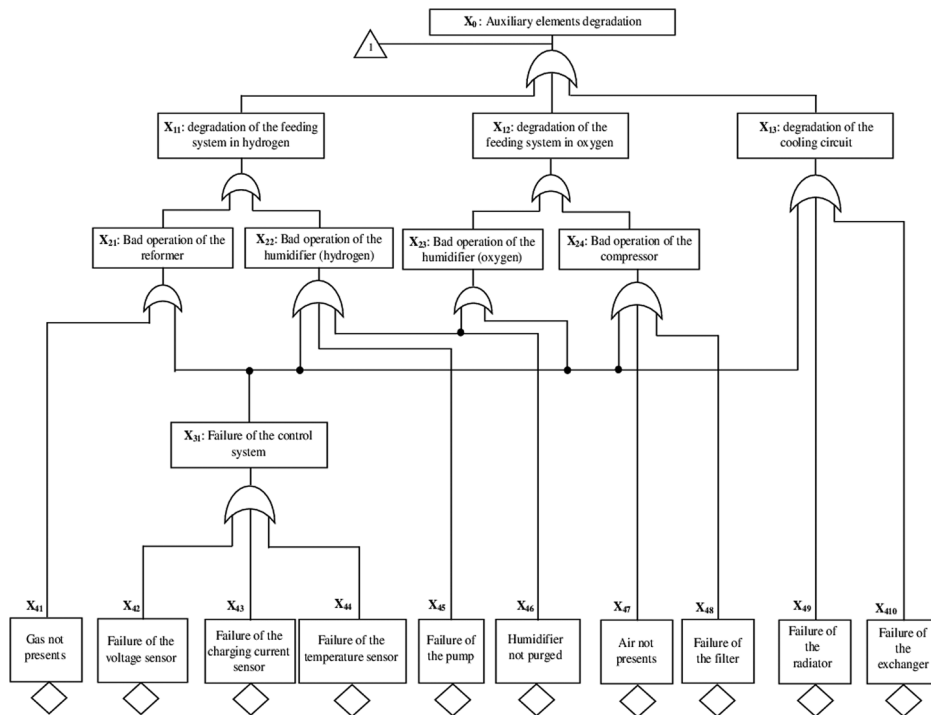


Fig. 3 Causal tree of fuel cell system

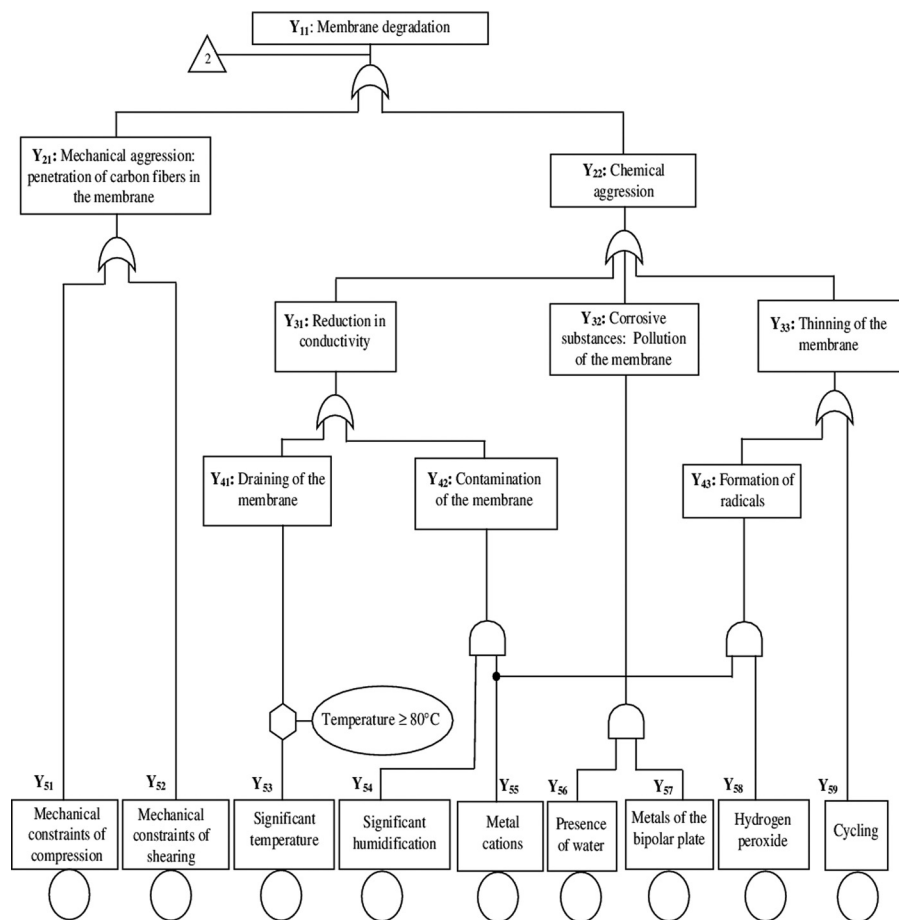


Fig. 4 Causal tree of membrane

Top events: The degradation of the fuel cell system is the top event of the causal tree. This event noted Z_0 is single for the causal tree and is at the “top” of the tree.

Z_0 : fuel cell system degradation.

Intermediate events: They present the different combinations of events that can lead to generate the top event.

X_0 : auxiliary elements degradation, Y_0 : fuel cell degradation, X_{11} : degradation of the feeding system in hydrogen, X_{12} : degradation of the feeding system in oxygen, X_{13} : degradation of the cooling circuit, X_{21} : bad operation of the reformer, X_{22} : bad operation of the humidifier (hydrogen), X_{23} : bad operation of the humidifier (oxygen), X_{24} : bad operation of the compressor, X_{31} : failure of the control system, Y_{11} : membrane degradation, Y_{12} : electrode degradation, Y_{21} : mechanical aggression—penetration of carbon fibers in the membrane, Y_{22} : chemical aggression, Y_{23} : reduction in active surface, Y_{24} : poisoning of the anode catalyst, Y_{31} : reduction in conductivity, Y_{32} : corrosive substances—pollution of the membrane, Y_{33} : thinning of the membrane, Y_{34} : degradation of the binder, Y_{35} : agglomeration, Y_{41} : draining of the membrane, Y_{42} : contamination of the membrane, and Y_{43} : formation of radicals.

Elementary events: Basic events at the bottom of the causal tree that present the causes of failures origin.

X_{41} : gas is not present, X_{42} : failure of the voltage sensor, X_{43} : failure of the charging current sensor, X_{44} : failure of the temperature sensor, X_{45} : failure of the pump, X_{46} : humidifier not purged, X_{47} : air not presents, X_{48} : failure of the filter, X_{49} : failure of the radiator, X_{410} : failure of the exchanger, Y_{51} : mechanical constraints of compression, Y_{52} : mechanical constraints of shearing, Y_{53} : significant temperature, Y_{54} : significant humidification, Y_{55} : metal cations, Y_{56} : presence of water, Y_{57} : metals of the bipolar plate, Y_{58} : hydrogen peroxide, Y_{59} : cycling, Y_{510} : significant pressure of gases, and Y_{511} : carbon monoxide.

$Rs(t)$ reliability is the probability so that the fuel cell system functions between $[0, t]$, that is, the event Z_0 does not occur.

$$Rs(t) = 1 - P(Z_0) = 1 - P(X_0 \cup Y_0) \quad (1)$$

$$P(Z_0) = P(X_0) + P(Y_0) - P(X_0 \cap Y_0) \quad (2)$$

The probability of the auxiliary elements degradation is

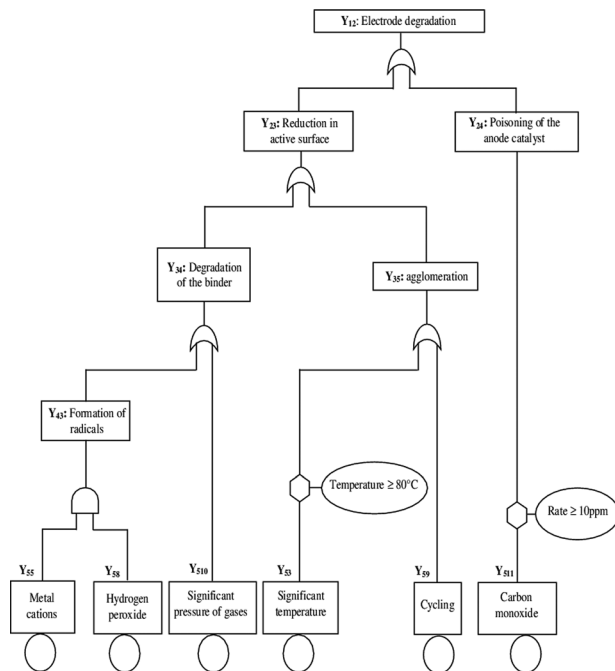


Fig. 5 Causal tree of electrode

$$P(X_0) = P(X_{11} \cup X_{12} \cup X_{13}) \quad (3)$$

The probability of the degradation of the feeding system in hydrogen is

$$P(X_{11}) = P(X_{21} \cup X_{22}) \quad (4)$$

The probability of the degradation of the feeding system in oxygen is

$$P(X_{12}) = P(X_{23} \cup X_{24}) \quad (5)$$

The probability of the degradation of the cooling circuit is

$$P(X_{13}) = P(X_{31} \cup X_{49} \cup X_{410}) \quad (6)$$

The probability of the bad operation of the reformer is

$$P(X_{21}) = P(X_{41} \cup X_{31}) \quad (7)$$

The probability of the bad operation of the humidifier (hydrogen) is

$$P(X_{22}) = P(X_{31} \cup X_{45} \cup X_{46}) \quad (8)$$

The probability of the bad operation of the humidifier (oxygen) is

$$P(X_{23}) = P(X_{31} \cup X_{46}) \quad (9)$$

The probability of the bad operation of the compressor is

$$P(X_{24}) = P(X_{31} \cup X_{47} \cup X_{48}) \quad (10)$$

The probability of the failure of the control system is

$$P(X_{31}) = P(X_{42} \cup X_{43} \cup X_{44}) \quad (11)$$

The probability of the fuel cell is

$$P(Y_0) = P(Y_{11} \cup Y_{12}) = P(Y_{11}) + P(Y_{12}) - P(Y_{11} \cap Y_{12}) \quad (12)$$

The probability of the membrane degradation is

$$P(Y_{11}) = P(Y_{21} \cup Y_{22}) \quad (13)$$

The probability of the electrode degradation is

$$P(Y_{12}) = P(Y_{23} \cup Y_{24}) \quad (14)$$

The probability of the mechanical aggression—penetration of carbon fibers in the membrane is

$$P(Y_{21}) = P(Y_{51} \cup Y_{52}) \quad (15)$$

The probability of the chemical aggression is

$$P(Y_{22}) = P(Y_{31} \cup Y_{32} \cup Y_{33}) \quad (16)$$

The probability of the reduction in active surface is

$$P(Y_{23}) = P(Y_{34} \cup Y_{35}) \quad (17)$$

The probability of the anode catalyst poisoning is

$$P(Y_{24}) = P(Y_{511}) \quad (18)$$

The probability of the reduction in conductivity is

$$P(Y_{31}) = P(Y_{41} \cup Y_{42}) \quad (19)$$

The probability of the membrane pollution is

$$P(Y_{32}) = P(Y_{56} \cup Y_{57}) \quad (20)$$

The probability of the membrane thinning is

$$P(Y_{33}) = P(Y_{43} \cup Y_{59}) \quad (21)$$

The probability of the binder degradation is

$$P(Y_{34}) = P(Y_{43} \cup Y_{510}) \quad (22)$$

The probability of the agglomeration

$$P(Y_{35}) = P(Y_{53} \cup Y_{59}) \quad (23)$$

The probability of the membrane draining

$$P(Y_{41}) = P(Y_{53}) \quad (24)$$

The probability of the membrane contamination

$$P(Y_{42}) = P(Y_{54} \cup Y_{55}) \quad (25)$$

The probability of the formation of radicals

$$P(Y_{43}) = P(Y_{55} \cup Y_{58}) \quad (26)$$

The most significant factors on the degradation of the fuel cell are: F_{P1} : temperature, F_{P2} : flow of hydrogen, F_{P3} : air flow, F_{P4} : hydrogen pressure, and F_{P5} : air pressure.

If each factor is characterized by two levels, min and max, then the experimental design requires 32 different experiments, and the mean time between failures MTBF is determined by the following equation:

$$\begin{aligned} \text{MTBF} = \overline{\text{MTBF}} + E_{P1}F_{P1} + E_{P2}F_{P2} + E_{P3}F_{P3} \\ + E_{P4}F_{P4} + E_{P5}F_{P5} + \text{effects of correlation} \end{aligned} \quad (27)$$

with

$$E_p = [E_{P1} \ E_{P2} \ E_{P3} \ E_{P4} \ E_{P5}]^T : \text{vector of the effects}$$

The following equation presents the probability that event Y_{5j} is at the origin of the Y_0 occurrence:

$$P(Y_{5j}/Y_0) = \frac{P(Y_{5j})P(Y_0/Y_{5j})}{\sum_{i=1}^n P(Y_{5i})P(Y_0/Y_{5i})} \quad (28)$$

where Y_{5i} is the assembly of elementary events and $P(Y_{5j})$ is the occur probability of the event Y_{5j} .

The theoretical occurs probabilities of the events Y_{5j} are naturally unknown. The probability law used to evaluate the fuel cell reliability is the Weibull law. This law is mainly used to characterize the materials comportment for all their life period. Weibull probability density function is

$$f(t) = \frac{\beta_j(t - \gamma_j)^{\beta_j-1}}{\eta_j^{\beta_j}} \exp - \left(\frac{t - \gamma_j}{\eta_j} \right)^{\beta_j} \quad (29)$$

An exploitation database is necessary to calculate the parameters of the Weibull law. In absence of this database, the authors propose to analyze the reliability by the variation parameters of the fuel cell model.

3 Fault Tree Analysis

The causal tree developed previously is completed by a fault tree analysis elaborated with using the elements of the fuel cell model. Therefore, it is thus necessary to know which parameters will influence the starting of the degradation modes (electrode degradation and membrane degradation).

3.1 Fuel Cell Model. The model is developed specifically for studying the depth degradation of the fuel cell as described in Eqs. (30)–(32). These equations present the description of the dynamics evolution of the fuel cell. Note the presence of three input variables, which are the hydrogen inlet flow, the oxygen inlet flow, and the density of current. The output variables on the side of cathode are the partial pressure of hydrogen, oxygen, and water [17,18]

$$\frac{dp_{H_2}}{dt} = \frac{RT}{V_A} (H_{2_{inlet}} - H_{2_{used}} - H_{2_{outlet}}) \quad (30)$$

$$\frac{dp_{O_2}}{dt} = \frac{RT}{V_C} (O_{2_{inlet}} - O_{2_{used}} - O_{2_{outlet}}) \quad (31)$$

$$\frac{dp_{H_2O_C}}{dt} = \frac{RT}{V_C} (H_{2O_{C_{inlet}}} - H_{2O_{C_{produced}}} - H_{2O_{C_{outlet}}}) \quad (32)$$

where $H_{2_{inlet}}$, $O_{2_{inlet}}$, and $H_{2O_{C_{inlet}}}$ are the inlet flow rates of hydrogen, oxygen, and water of the electrode; $H_{2_{outlet}}$, $O_{2_{outlet}}$, and $H_{2O_{C_{outlet}}}$ are the outlet flow rates of each gas and water vapor; and $H_{2_{used}}$, $O_{2_{used}}$, and $H_{2O_{C_{produced}}}$ are the usage and production of the gases and water.

By basing on the basic electrochemical relations, the production of gases is related to the output current by the following equation:

$$H_{2_{used}} = 2O_{2_{used}} = 2KI = 2KA_C i \quad (33)$$

with $K = N/4F$, A_C is the active area, and i is the current density.

The following equation describes the fuel cell model:

$$\begin{pmatrix} \dot{x}_1 \\ \dot{x}_2 \\ \dot{x}_3 \end{pmatrix} = \begin{pmatrix} \frac{RT}{V_A} \left(1 - \frac{x_1}{P_{op}} \right) & 0 & \frac{RT}{V_A P_{op}} (-2KA_C + 2KA_C x_1) \\ 0 & \frac{RT}{V_C} \left(1 - \frac{x_2}{P_{op}} \right) & \frac{RT}{V_C P_{op}} (-KA_C + KA_C x_2) \\ 0 & \frac{RT}{V_C P_{op}} & \frac{RT}{V_C P_{op}} (-2KA_C - 2KA_C x_3) \end{pmatrix} \times \begin{pmatrix} u_1 \\ u_2 \\ u_3 \end{pmatrix} \quad (34)$$

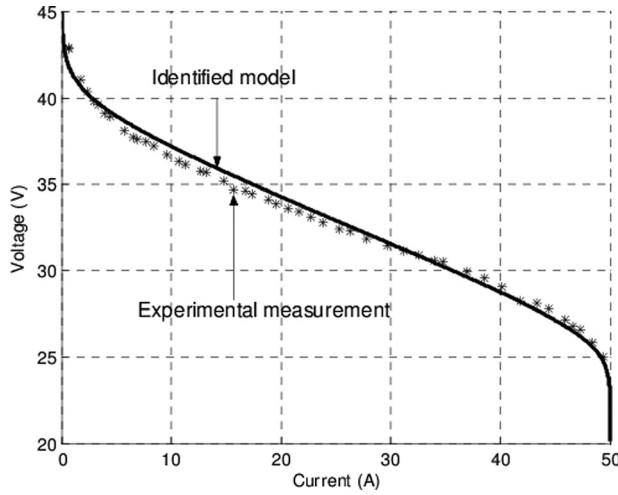


Fig. 6 Output characteristic of Nexa cell fuel

where

$$\begin{pmatrix} x_1 \\ x_2 \\ x_3 \end{pmatrix} = \begin{pmatrix} P_{H_2} \\ P_{O_2} \\ P_{H_2O_c} \end{pmatrix} \quad (35)$$

$$\begin{pmatrix} u_1 \\ u_2 \\ u_3 \end{pmatrix} = \begin{pmatrix} H_{2inlet} \\ O_{2inlet} \\ i \end{pmatrix} \quad (36)$$

3.2 Parameters Identification of the Fuel Cell Model. The parameters identification of the fuel cell model is carried out with experimental measurements of the output characteristic at the beginning of life of the Nexa fuel cell model 310-002702, 1.2 kW. The output voltage varies with power, ranging from about 43 V at system idle to about 26 V at full load. Figure 6 illustrates the fuel cell output characteristic resulting from experimental statements; it was raised by measuring the current and the terminal voltage for various values of load resistance.

Some factors produce voltage drops in a fuel cell. Such losses will cause the cell voltage to be less than its ideal potential. These losses are generated by irreversibility and they appear in three elements: activation losses, Ohmic losses, and concentration losses.

According to the Nernst equation and the voltage drops, the fuel cell voltage is described as

$$V = N \left(E^0 + \frac{RT}{2F} \ln \left\{ \frac{P_{H_2} (P_{O_2}/P_{std})^{1/2}}{P_{H_2O}} \right\} - \Delta V \right) \quad (37)$$

where V is the output voltage, N is the number of cells, E^0 is the cell open circuit voltage, T is the operating temperature, ΔV is the voltage loss, P_{H_2} , P_{O_2} , and P_{H_2O} are the partial pressures of each gas inside cell, R is the gas constant, and P_{std} is the standard pressure.

The fuel cell drop voltage is given in Eq. (38). These voltage drops allow identifying the parameters of the fuel cell model

$$\Delta V = \Delta V_R + \Delta V_A + \Delta V_C \quad (38)$$

Table 1 Estimated parameters of the fuel cell model

Area specific resistance	$r = 0.43 \, \Omega \cdot \text{cm}^2$
Charge transfer coefficient	$\alpha = 0.5 \rightarrow A = 0.0291$

The Ohmic losses ΔV_R occur due to the resistance to electron flow in the bipolar plates

$$\Delta V_R = r \cdot i \quad (39)$$

where i is the current density and r is the area specific resistance.

The activation losses ΔV_A are predominantly due to the kinetics at the electrodes

$$\Delta V_A = A \ln \left(\frac{i}{i_0} \right) \text{ with } A = \frac{RT}{2\alpha F} \quad (40)$$

where α is the charge transfer coefficient and i_0 is the exchange current.

The concentration losses ΔV_C are the result from the decrease partial pressure compared to the reference pressure

$$\Delta V_C = -B \ln \left(1 - \frac{i}{i_L} \right) \text{ with } B = \frac{RT}{2F} \quad (41)$$

Model parameters used in identification of our simulation are given as follows:

- fuel cell active area: $A_C = 100 \, \text{cm}^2$
- anode volume: $V_A = 6.5 \, \text{cm}^3$
- cathode volume: $V_C = 12 \, \text{cm}^3$
- number of cells: $N = 47$
- operating pressure: $P = 101 \, \text{kPa}$
- operating cell temperature: $T = 338 \, \text{K}$
- cell open circuit voltage: $E_0 = 0.6 \, \text{V}$

As shown in Fig. 6, the output characteristic presents a voltage drop. These voltage drops allow identifying the parameters of the fuel cell model (Table 1). The output characteristic of the fuel cell model identified through the estimated parameters also gives results similar to the real measurements.

3.3 Interval of Parameters Variation of the Fuel Cell Model. To build the fault tree analysis, authors analyze the influence of each degradation mode on the variation of the parameters of the fuel cell model. During the life cycle, the parameters of the fuel cell model vary and cause its aging. In fact, these variations produce the augmentation in the internal impedance and the raise

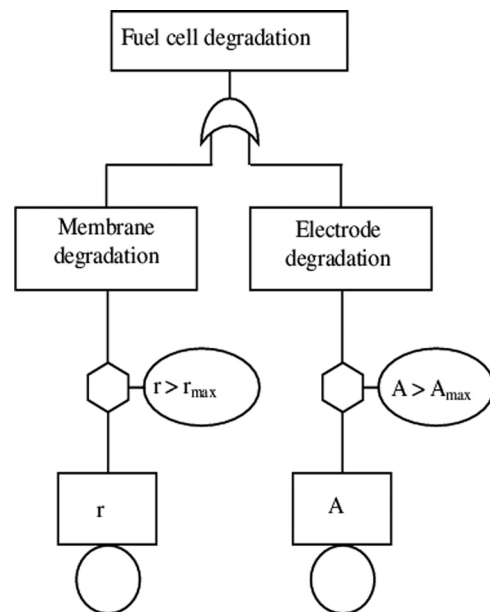


Fig. 7 Fault tree analysis of the fuel cell degradation

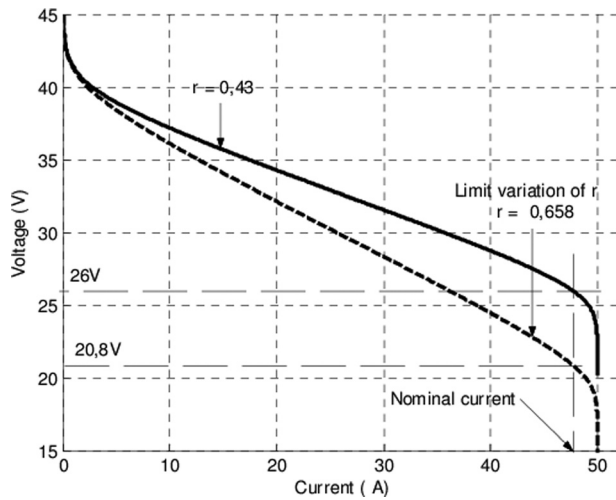


Fig. 8 Limit variation of r ($0.43 \leq r \leq 0.658$)

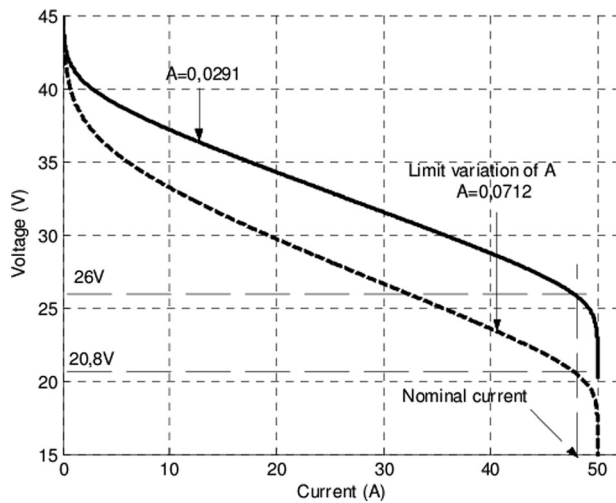


Fig. 9 Limit variation of A ($0.0291 \leq A \leq 0.0712$)

in the voltage drops. Figure 7 presents the different variations of parameters and their effects on fuel cell degradation.

The membrane degradation generates the variation of the area specific resistance (r), and the electrode degradation generates the variation of the charge transfer coefficient (α). The determination of upper limit of the fuel cell parameters model is particularly advantageous, since it helps to determine the depth of degradation. The lifetime of the fuel cell is achieved when its nominal voltage falls of 20% for the nominal current. These limits are given for a minimum voltage generated by the fuel cell, which is of 80% of its nominal voltage.

Figures 8 and 9 present the results of output characteristic simulation, which show the respective limits r_{\max} and A_{\max} when each failure mode is taken independently.

Table 2 Intervals of parameters variation

Parameters of the fuel cell model	Values at beginning of life of the fuel cell	Values limit	Intervals of variation limit
r ($\Omega \cdot \text{cm}^2$)	0.43	0.658	$\Delta r_{\max} = 0.228$
A	0.0291	0.0712	$\Delta A_{\max} = 0.0421$

Table 2 shows the maximum intervals of parameters variation Δr_{\max} and ΔA_{\max} . The difference between the parameters limits values of a degraded fuel cell and the parameters at the beginning of life allows us to calculate the maximum intervals. The parameters variations of the fuel cell model and their effects on degradation are shown in Fig. 10.

4 Failure Detectability

The failures detectability presented in Fig. 11 is based on the comparison of the experimental output characteristic at beginning of life of the fuel cell to the used fuel cell. The extraction of the parameters r and A of the experimental response of the fuel cell used allows to calculate the variation intervals and the coefficients α_1 and α_2 . These coefficients give information about the lifetime and the depth degradation of the fuel cell. This approach determines the impact of each degradation mode (membrane degradation and electrode degradation).

A fuel cell is degraded by the superposition of the various degradation modes (membrane degradation and electrode degradation). Figure 12 presents the experimental output characteristic of the used fuel cell. A parametric identification of r and A was carried out. Then, the variations $\Delta r_{\text{measured}}$ and $\Delta A_{\text{measured}}$ of a used fuel cell are calculated and then compared to the variations parameters at the beginning of life of a fuel cell.

Coefficients α_1 and α_2 present the percentage of each mode of degradation.

α_1 presents the percentage of membrane degradation

$$\alpha_1 = 100 \frac{\Delta r_{\text{measured}}}{\Delta r_{\max}} \quad (42)$$

α_2 presents the percentage of electrode degradation

$$\alpha_2 = 100 \frac{\Delta A_{\text{measured}}}{\Delta A_{\max}} \quad (43)$$

The several degrees of degradation relating to each failure mode are summarizes in Table 3. The sum $\alpha_1 + \alpha_2$ indicates the aging of fuel cell, it is supposed degraded if the sum exceeds

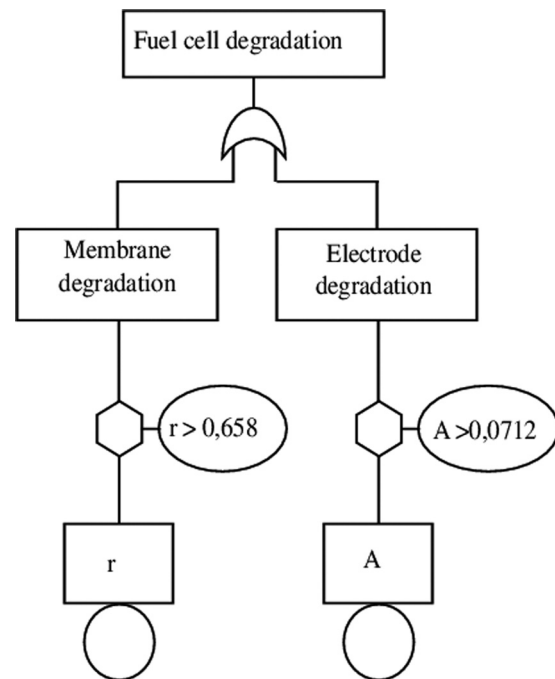


Fig. 10 Fault tree analysis of the deficiency presenting the limiting values

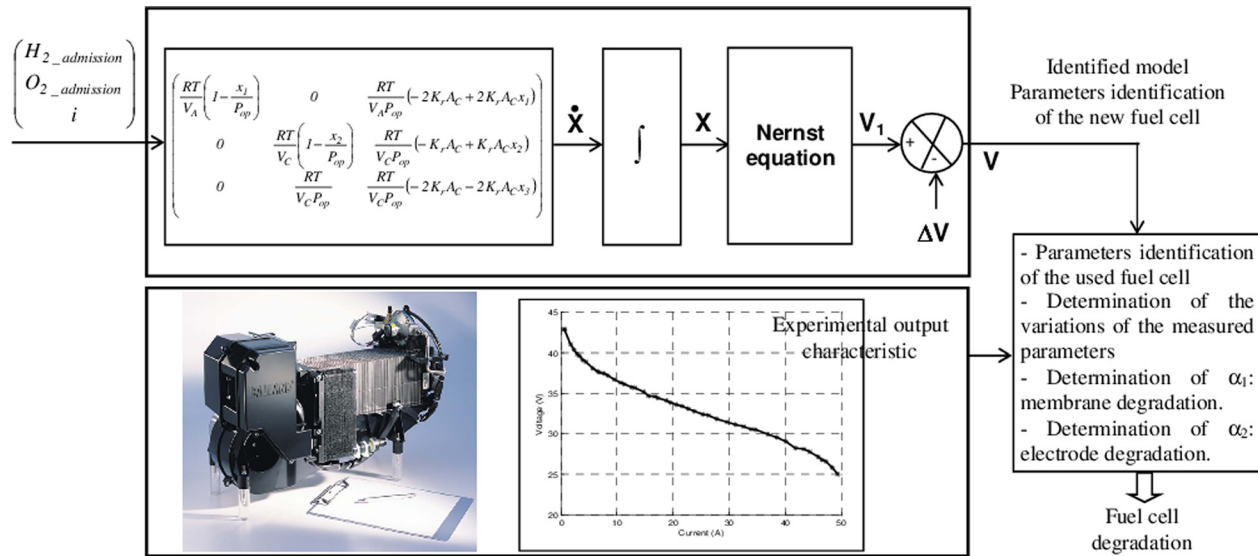


Fig. 11 Synoptic diagram of the diagnosis system

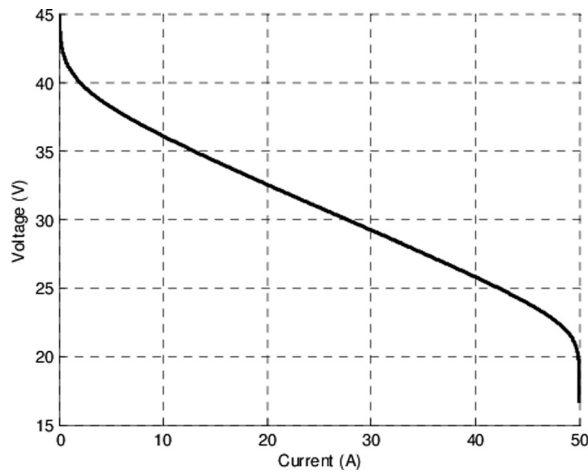


Fig. 12 Output characteristic of the used Nexa cell fuel

Table 3 Aging of fuel cell

α_1 (%)	48.24
α_2 (%)	9.5
Parameter variation (%)	57.74
Aging of fuel cell	Fuel cell nondegraded

100%. Finally, the results show that the proposed method is a remarkable tool for diagnosis and compensatory action of the fuel cell.

5 Conclusions

In this paper, a detailed approach is developed to describe the influence of the operation conditions on the conditions inside the fuel cell and understanding of the degradation processes. This approach is based on the research of the various phenomena causing the reduction in the performances of the proton exchange membrane fuel cell. A causal tree describing the origin of proton exchange membrane fuel cell deficiency and a fault tree analysis allows to study the degradation by examination the parameters variation of the equivalent model. The execution of the diagnosis based on dependability tools allows to qualify and quantify the

degree of each degradation mode and to judge the state of the fuel cell lifetime.

References

- [1] Sirisukprasert, S., and Saengsuwan, T., 2008, "The Modeling and Control of Fuel Cell Emulators," *ECTI-CO*, **2008**, pp. 985–988.
- [2] Blunier, B., and Miraoui, A., 2008, "Modelling of Fuel Cells Using Multi-Domain VHDL-AMS Language," *J. Power Sources*, **177**(1), pp. 434–450.
- [3] Tounthong, P., Sadli, I., Raël, S., and Davat, B., 2006, "A Control Strategy of Fuel Cell/Battery Hybrid Power Source for Electric Vehicle Applications," 37th IEEE Power Electronics Specialists Conference (PESC '09), Jeju, Korea, June 18–22.
- [4] Le Ny, M., 2013, "Current Distribution Identification in Fuel Cell Stacks From External Magnetic Field Measurements," *IEEE Trans. Magn.*, **49**(5), pp. 1925–1929.
- [5] Fouquet, N., Doulet, C., Nouillant, C., Dauphin-Tanguy, G., and Ould-Bouamama, B., 2006, "Model Based PEM Fuel Cell State-of-Health Monitoring Via AC Impedance Measurements," *J. Power Sources*, **159**(2), pp. 905–913.
- [6] Nakajima, H., Konomi, T., Kitahara, T., and Tachibana, H., 2008, "Electrochemical Impedance Parameters for the Diagnosis of a Polymer Electrolyte Fuel Cell Poisoned by Carbon Monoxide in Reformed Hydrogen Fuel," *ASME J. Fuel Cell Sci. Technol.*, **5**(4), p. 041013.
- [7] Majdara, A., and Wakabayashi, T., 2009, "Component-Based Modeling of Systems for Automated Fault Tree Generation," *Reliab. Eng. Syst. Saf.*, **94**(6), pp. 1076–1086.
- [8] Rasool, K., 1991, "Event-Tree Analysis by Fuzzy Probability," *IEEE Trans. Reliab.*, **40**(1), pp. 120–124.
- [9] Brik, K., and Ben Ammar, F., 2013, "Causal Tree Analysis of Depth Degradation of the Lead Acid Battery," *J. Power Sources*, **228**, pp. 39–46.
- [10] Song, Y., Han, S. B., Park, S. I., Jeong, H. G., and Jung, B. M., 2007, "A Power Control Scheme to Improve the Performance of a Fuel Cell Hybrid Power," IEEE Power Electronics Specialists Conference (PESC 2007), Orlando, FL, June 17–21, pp. 1261–1266.
- [11] Tirnovan, R., Giurgea, S., Miraoui, A., and Cirrincione, M., 2008, "Surrogate Modelling of Compressor Characteristics for Fuel Cell Applications," *Appl. Energy*, **85**(5), pp. 394–403.
- [12] Schmittinger, W., and Vahidi, A., 2008, "A Review of the Main Parameters Influencing Long-Term Performance and Durability of PEM Fuel Cells," *J. Power Sources*, **180**(1), pp. 1–14.
- [13] Taniguchia, A., Akita, T., Yasuda, K., and Miyazaki, Y., 2008, "Analysis of Degradation in PEMFC Caused by Cell Reversal During Air Starvation," *Int. J. Hydrogen Energy*, **33**(9), pp. 2323–2329.
- [14] Endoh, E., Terazono, S., Widjaja, H., and Takimoto, Y., 2004, "Degradation Study of MEA for PEMFCs Under Low Humidity Conditions," *J. Electrochem. Solid State*, **7**(7), pp. 209–211.
- [15] Jinfeng, W., Xiao, Z., Wanga, H., Zhang, J., Shena, J., Wua, S., and Merida, W., 2008, "A Review of PEM Fuel Cell Durability: Degradation Mechanisms and Mitigation Strategies," *J. Power Sources*, **148**(1), pp. 104–119.
- [16] Bi, W., and Fullera, B., 2007, "Temperature Effects on PEM Fuel Cells Pt Catalyst Degradation," *ECS Trans.*, **11**(1), pp. 1235–1246.
- [17] Woonki, N., Bei, G., and Bill, D., 2005, "Nonlinear Control of PEM Fuel Cells by Exact Linearization," *Ind. Appl. Conf.*, **4**(2–6), pp. 2937–2943.
- [18] Jia, J., Wang, Y., and Lian, D., 2008, "Matlab/Simulink Based-Study on PEM Fuel Cell and Battery Hybrid System," 10th International Conference on Control, Automation, Robotics and Vision (ICARCV 2008), Hanoi, Vietnam, Dec. 17–20, pp. 2108–2113.